Int. J. Heat Mass Transfer. Vol. 18, pp. 51–60. Pergamon Press 1975. Printed in Great Britain

BOILING HEAT TRANSFER TO A FREON-113 JET IMPINGING UPWARD ONTO A FLAT, HEATED SURFACE

M. A. RUCH
Q-Dot Corporation, Dallas, Texas 75247, U.S.A.

and

J. P. HOLMAN
Mechanical Engineering Department, Southern Methodist University, Dallas, Texas 75275, U.S.A.

(*Received* 15 *September* 1973 *and in revised form* 14 *May* 1974)

Abstract—Experimental measurements of the heat transfer and heat flux to a jet impinging on a heated test surface were obtained in the nucleate and film boiling regimes. Test variables were jet nozzle inside diameter, test surface orientation, and test surface temperature. A generalized correlation of the jet nucleate boiling heat flux was found using a modified form of the Rohsenow pool boiling equation. For Freon-113, dimensional correlations of the heat transfer and heat flux data in both nucleate and film boiling were obtained in terms of the four test variables.

NOMENCLATURE

A, area of fluid–solid contact; heat-transfer area [ft^2];
c_p, specific heat at constant pressure [Btu/1bm-°F];
C_{sf}, experimentally determined constant dependent on the fluid–surface combination; appears in Rohsenow correlation, equation (7) [dimensionless];
D, needle, or nozzle, inside diameter [ft];
g, local acceleration of gravity [ft/h^2];
g_c, conversion constant [$4{\cdot}17 \times 10^8$ ft-1bm/1bf-h^2];
H, mean height of climb [in];
k, thermal conductivity [Btu/h-ft-°F];
$\dot{m}$, mass flow rate [1bm/h];
P, power consumed by heater [Btu/h];
Pr, Prandtl number ($\mu c_p/k$) [dimensionless];
Q, net heat transfer [Btu/h];
Q/A, net heat flux; net heat transfer divided by average area of fluid–solid contact [Btu/h-ft^2];
Q_a, environmental heat loss from heater [Btu/h];
Re, Reynolds number ($\rho VD/\mu$) [dimensionless];
T_s, surface temperature [°F];
ΔT_x, saturation temperature excess; surface temperature minus saturation temperature [°F];
V, jet velocity [ft/h];
We, Weber number ($\rho V^2 D/\sigma g_c$) [dimensionless].

Greek symbols
μ, absolute viscosity [1bm/h-ft];
ρ, density [1bm/ft^3];
σ, surface tension [1bf/ft];
θ, heater orientation angle [degrees].

Subscripts
f, saturated liquid;
v, saturated vapor.

INTRODUCTION

BECAUSE of the high heat removal rates that can often be achieved by evaporation, this method of cooling is attractive for use in industry. One form of evaporative cooling that has potential industrial application for localized cooling is the boiling of a liquid jet impinging on a high temperature surface. Prior to proper evaluation of its potential as a cooling technique, however, a thorough qualitative and quantitative understanding of the phenomena which govern jet boiling must be obtained.

Although considerable effort has been spent on boiling investigations, as well as extensive research on single phase jets, there has been very little done with the combination phenomenon of jet boiling. Boiling research has logically been separated into the two regimes: nucleate boiling and film boiling. In both regimes major interest has centered on free and forced convection in extensive liquid masses, and forced convection in tubes. Most of the work in nucleate boiling has been experimental in nature, while film boiling efforts seem to be more equally divided between theoretical and experimental analyses. Research on the fluid mechanics of jet flows without phase change is extensive, and has primarily been carried out with air as the jet fluid.

The most extensive work to date on the boiling of a jet is that of Copeland [4], who experimentally investigated the steady state behavior of a circular water jet flowing vertically upward onto a horizontal, flat, heated surface. The surface was a circular, nickel-plated, copper surface with a $\frac{3}{4}$-in dia. Results were obtained in both the nucleate and film boiling regimes. Because of scaling problems, the data scatter was so great as to preclude any correlation of the film boiling data. In the nucleate boiling regime, the net heat transfer to the jet and the net heat flux were found to be dependent only on the temperature excess, defined as the difference between the surface temperature and the saturation temperature. No dependency was found on jet impact velocity, jet diameter or jet temperature. In nucleate boiling, the surface area covered by the jet was the entire test surface, and the water was observed to climb the side surface of the cylinder. Data scatter in the nucleate boiling regime was on the order of 40 per cent, probably due to scaling deposits on the test surface.

The transient boiling of jets incident on flat plates initially heated to 1050°C was the subject of experimental research conducted by Akimenko [1]. Velocities up to 30 m/s were employed for water jets at 20°C. The results were plotted in the form of the "second critical" heat flux defined as the minimum heat flux prior to stable film boiling vs jet velocity. The greatest value of "second critical" heat flux was found to occur at the highest jet velocity. Values of the "second critical" heat flux ranged from 139×10^3 to 557×10^3 W/m^2.

Nevins [9] experimentally investigated jet boiling using water and several oils in a Jominy end-quench test, with surface temperatures ranging from 120 to 1200°F. The jet velocity was maintained at approximately 3 ft/s, and the jet liquid temperatures varied between 85 and 100°F. A steady state technique was employed to yield heat-transfer coefficients in the surface temperature range of 120–380°F, while a transient method was utilized over the range 400–1200°F. The results obtained from the two methods differed by a factor of almost two at a surface temperature of 350°F. The inherent transient nature of the impinging jet was postulated to be the source of the observed difference.

It was apparent from the literature search that little was known about the heat-transfer characteristics of steady-state jet boiling and that a contribution could be made in this area. An experimental research program was then established to determine the effect on steady state jet boiling heat transfer and heat flux with variation of the following parameters: (a) jet velocity; (b) jet nozzle inside diameter; (c) surface temperature; and (d) heater surface orientation.

In order to minimize heat transfer by run-off liquid, the jet was directed vertically upward to impinge on a downward-facing, flat, heated surface. Freon-113 (Trichlorotrifluorethane) was chosen as the test liquid because of its thermophysical properties, particularly its low boiling impurities, and availability of property data. All Freon-113 properties shown in this work are from [2, 3 or 5]. The specific fluid employed was the commercial product of the E. I. Dupont Co.

EXPERIMENTAL APPARATUS AND METHODS

The experimental apparatus to accomplish the research goals consisted of three basic sections: the heater assembly, a flow supply system and jet nozzles. The heater assembly consists of two parts: a heater to provide a heated test surface, and leveling platform to allow variation of the test surface orientation. A schematic of the heater design is shown in Fig. 1. Dissipation of electric power through resistance heating elements causes the copper core to become heated, and this heat is supplied to the test surface by conduction in the copper.

Copper was chosen for the core material because of its high thermal conductivity and thermal diffusivity. The test surface was ground to a finish of 32 μin, and, the cylindrically symmetric copper core was plated with 0·0010 in of nickel to reduce radiation heat loss from the exposed portion and minimize surface corrosion. A thin layer of Sauereisen electrical insulating cement was applied to the area where the heating elements were to be wound. After the wires were installed, another thin layer of Sauereisen cement was applied. To minimize the heat losses from all portions of the copper core except the exposed portion, the non-exposed surfaces were then surrounded by Thermobestos thermal insulation. The copper core and insulation were placed in a $3 \times 3 \times 3$ in container of 0·05-in thick yellow brass to provide a relatively isothermal outside surface for the heater. The container was coated with aluminum paint to reduce radiation loss from its exterior.

The heating elements consisted of two 18 gauge Nichrome-V wires connected in series to yield a nominal total resistance of 4·1 Ω. Maximum design power rating of the heater was 2050 Btu/h. Power supply to the heating elements was controlled by two 2·6 kVA powerstats connected in series. This arrangement allowed very precise voltage control to the heating elements. The leveling platform provided a means of orienting the test surface at angles of 0, 15, 30, 45, 60, 75 and 90 degrees with respect to the horizontal.

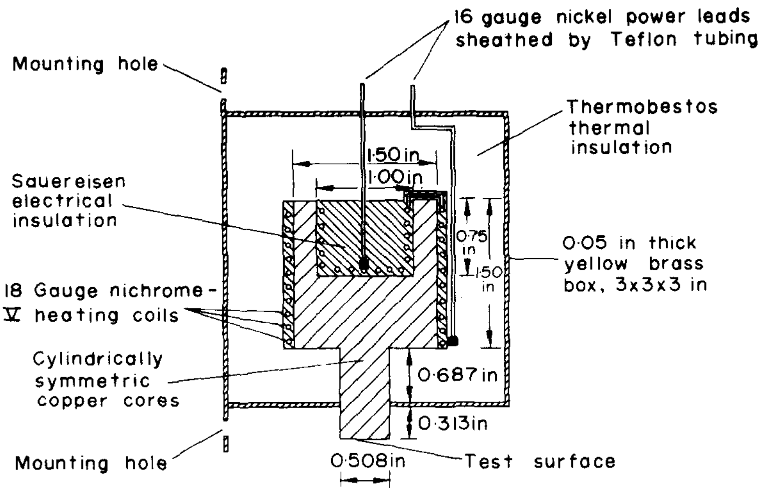

FIG. 1. Front cross-sectional view of heater.

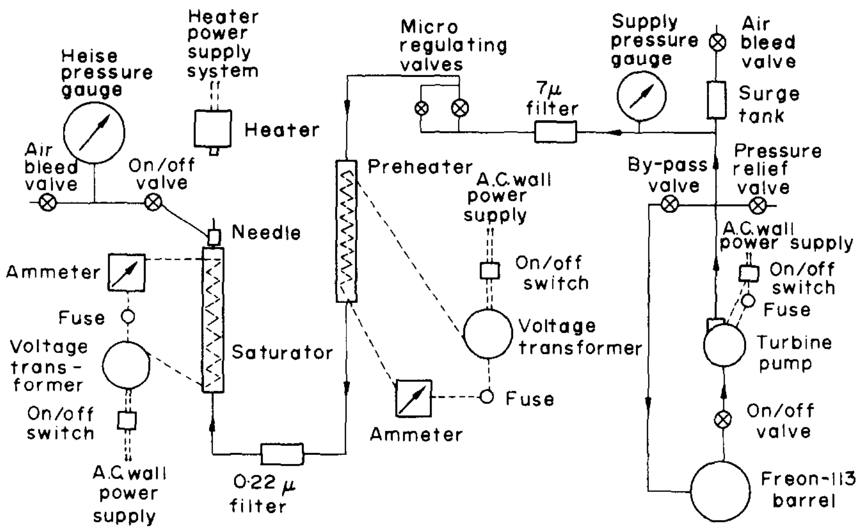

FIG. 2. Schematic of Freon-113 supply system.

Figure 2 presents the Freon-113 supply system in schematic form. Care was taken in selection of construction materials to minimize the possibility of system-added impurities to the Freon-113. All tubing was made of either copper, nylon, or teflon, and all valves and fittings were constructed of either brass or stainless steel. Two filters were also included in the flow system. The flow rate to the jet nozzle was controlled by setting the by-pass valve to obtain the desired supply pressure and then adjusting the two micro-regulating valves.

Electric resistance heating elements were installed in two places in the flow supply system to heat the Freon-113 to near saturation conditions at the jet nozzle. These two elements were called the preheater and the saturator. These elements were not used during the course of the experiments reported herein.

Standard medical hypodermic needles were employed as jet nozzles to accelerate the flow. Three different sizes were used: 27, 24 and 22 gauge. Each needle was pressed and soldered into an adapter with a $\frac{1}{4}$-in NPT male fitting. This fitting was then coupled with a $\frac{1}{4}$-in NPT female run tee, of which one branch connected to the Freon-113 supply and the other branch connected to a Heise pressure gauge for measurement of the pressure drop across the needle.

INSTRUMENTATION

Using 30 gauge iron–constantan thermocouples in conjunction with a potentiometric recorder, temperatures were measured at twelve places on the apparatus: seven thermocouples were peened into the copper heater core, three were soldered to the outside of the heater box, one was located at the jet nozzle outlet, and one was located upstream of the nozzle. The thermocouples were enclosed in plastic tubing to protect them from sprayed liquid.

No thermocouples were located on the test surface since these would distort the jet boiling. Instead, the seven thermocouples were located in low thermal gradient regions of the heater where they would produce minimum distortion of the temperature field in the heater. From these measurements the surface temperature could be computed. The thermocouple located closest to the surface ($\frac{7}{8}$-in away) was chosen for use as the basis of surface temperature measurement. The portion of the heater from the location of the closest thermocouple to the test surface was modelled with the NETHAN (Network Thermal Analyzer) program described by Reynard and Billerbeck [10]. The network consisted of sixty-three nodes connected by 106 thermal resistances, and the model included heat losses to the environment based on calibration data. Internal as well as surface nodal temperatures were calculated for seventeen different experimental jet heat flux conditions. From these data it was possible to establish an analytical relationship between the surface temperature at the jet and the temperature measured $\frac{7}{8}$-in from the surface. It is believed that the surface temperatures determined in this way are accurate within $\pm 4{\cdot}5$°F, considering all experimental uncertainties and calculation inaccuracies.

Thermobestos thermal insulation was placed around the jet nozzle assembly and this was then covered by a plastic sheet to prevent heat transfer to the assembly from run-off liquid. The temperature of the environment surrounding the test section was measured by a mercury-in-glass thermometer to an accuracy of 1°F.

The total AC power supplied to the heater was measured as the product of the total current flowing in the heater circuit times the voltage drop across the heater. The voltage drop was measured with a digital multimeter with an accuracy of 0·1 per cent of instrument reading +0·03 per cent of range. The total current flowing in the heater circuit was measured utilizing an ammeter with an accuracy of 0·2 per cent of full scale reading. Photographic techniques were employed to measure the heat-transfer area or area of contact of the fluid on the heating surface during boiling of the jet.

The inside diameter of each needle was determined within 3·0 per cent with a combination micrometer and microscope technique. The length of the needles were shortened so that each needle had a length to inside diameter ratio of approximately 63·9. Each of the three needles was positioned so that the ratio of distance from needle to the test surface divided by inside needle diameter was 22·6.

The mass flow rate, $\dot{m}$, through each needle was determined from a calibration of flow rate and pressure drop across the needle. The pressure drop was measured by a 0–150 psig Heise gauge accurate to within 0·1 per cent of full scale reading, or 0·15 psig. Once the mass flow rate was determined for a given test series, the corresponding mean jet velocity, V, was computed from

$$V = \frac{4\dot{m}}{\rho \pi D^2}. \tag{1}$$

For use in equation (1), the density was evaluated for liquid Freon-113 at 70°F. The Reynolds number at the nozzle outlet could then be calculated for each test series as:

$$Re = \frac{\rho V D}{\mu}. \tag{2}$$

Viscosity for use in equation (2) was evaluated at 70°F for liquid Freon-113.

The heat-transfer area, or area of contact, during boiling was obtained photographically. The diameter of the test surface, 0·508 in, was used as a reference to measure circular dimensions on the test surface. The exposed axial distance of the cylinder between the test surface and the heater box was 0·313 in and this dimension was utilized as a reference to measure the height of climb of liquid along the sides of the cylinder. Data were obtained by first measuring the length of the desired quantity and the reference dimension in the photograph. Then the desired dimension was linearly scaled using the above measurements and the reference dimension. The area of contact was then calculated assuming that the area was circular. When the liquid covered the entire test surface and then climbed the side surface of the cylinder the area of contact was computed as the sum of the test surface area and the area covered on the side of the cylinder.

Three pictures from different views were taken for each data run. Of these, generally at least two pictures were suitable for making area of contact calculations. An average area of contact for the data run was then obtained as the mean of the area of contacts from the individual pictures. The net heat transfer to the jet, Q, was calculated at steady-state conditions of the heater and jet by the following energy balance:

$$Q = P - Q_a \tag{3}$$

where P was the power input during boiling and Q_a was the environmental heat loss. The environmental heat loss of the heater was obtained from calibration of the power supplied to the heater at steady state with no jet flow but with all equipment in place. Once the net heat transfer was computed and the average area of contact computed, the net heat flux was given as the quotient, Q/A. The uncertainty in the heat flux was computed to nominally be 14·5 per cent in nucleate boiling without liquid climb, 2·2 per cent in nucleate boiling with liquid climb, and 28·9 per cent in film boiling. Most of this uncertainty results from the uncertainty in determination of the jet contact area.

RESULTS AND DISCUSSION

All experiments were run with the jet liquid temperature at approximately 70°F. Table 1 presents a summary of the range of variables covered during the course of the experiments. Because of the inherent differences in the phenomena occurring in the nucleate and film boiling regimes, these two regimes are treated separately in the following sections.

Table 1. Range of test variables

Variable	Range
Jet velocity, V	14 500–81 200 ft/h (1·23–6·87 m/s)
Needle inside diameter, D	0·00069–0·00142 ft (0·21–0·433 mm)
Heater orientation angle, θ	0–45 degrees
Surface temperature, T_s	133–725°F (56–385°C)
Heat transfer, Q	10·3–154·7 Btu/h (4·05–45·3 W)
Heat flux, Q/A	22 600–229 700 Btu/h-ft^2 (71·3–724·4 kW/m^2)
Saturation temperature excess, ΔT_x	15–608°F (8·33–338°C)
Jet Reynolds number, Re	1030–4120

Nucleate boiling

The nucleate boiling of a jet impinging onto a flat, heated surface is readily identified by the presence of vapor bubbles in the liquid on the test surface. In this sense, it is very similar to nucleate boiling in an extensive liquid pool. The onset of nucleate boiling occurred in the range of 24–29°F above saturation. Boiling crisis, or burnout as it is sometimes called, took place at a saturation temperature excess of approximately 80°F. Above this value, the rate of vapor generation became so great as to provide an insulating layer of vapor between the liquid and the surface, thus causing both the heat transfer and heat flux to decrease. A reduction in power supply to the heater was then necessary to prevent burnout of the heating coils.

The phenomena identified by Copeland [4] as "area expansion", in which the liquid covered all of the test surface and then climbed the vertical sides of the cylinder, was observed in the present research during only six runs, all of them during the same test series. This test series was performed at the highest mass flow rate ($\dot{m} = 6{\cdot}0$ lbm/h), but not at either the largest jet velocity or nozzle inside diameter. Of these six runs, only three were in the nucleate boiling regime; the other three runs were in the free convection boiling regime ($\Delta T_x < 24$°F). In all other nucleate boiling data runs, the area covered by the liquid after the jet impinged upon the surface, defined as the area of contact, A, was less than or equal to the area of the test surface.

The major flow pattern observed during nucleate boiling is depicted in Fig. 3. This flow pattern was also observed for boiling of a water jet on a downward-facing surface by Copeland [4]. As shown in Fig. 3, vigorous bubbling occurred everywhere on the test surface except near the point of jet impingement, where the liquid depth (measured downward from the test surface) was depressed from that of the surrounding liquid.

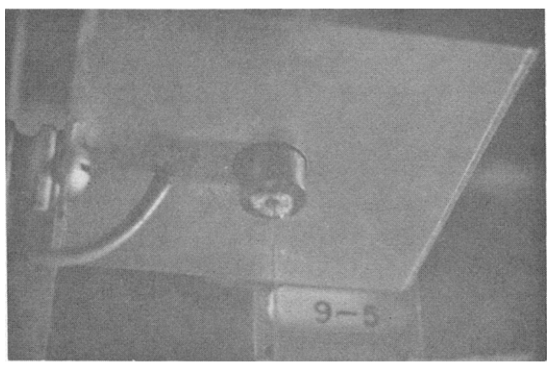

FIG. 3. Photographic view of nucleate boiling. $V = 14\,500$ ft/h (1·23 m/s); $D = 0{\cdot}00142$ ft (0·433 mm); $\theta = 0$ degrees; $Q = 42{\cdot}3$ Btu/h (12·39 W); $Q/A = 67\,200$ Btu/h-ft^2 (211·9 kW/m^2); $\Delta T_x = 49$°F (27·2°C).

The nucleate boiling heat-transfer data for Freon-113 are correlated within ±27 per cent as shown in Fig. 4 by the equation:

$$QV^{-1\cdot3}D^{-2\cdot0} = 2{\cdot}55(\Delta T_x)^{0\cdot85}. \qquad (4)$$

The nucleate boiling heat flux data were correlated as shown in Fig. 5, with a scatter of approximately ±35 per cent. The resulting equation for heat flux is

$$Q/A = 47{\cdot}1(\Delta T_x)^{1\cdot95}. \qquad (5)$$

Division of equation (4) by equation (5) yields an empirical expression for the jet contact area A

$$A = 0{\cdot}0541\, V^{1\cdot3}D^{2\cdot0}(\Delta T_x)^{-1\cdot10}. \qquad (6)$$

Four test series were run over a wide range of surface temperatures at constant jet nozzle diameter

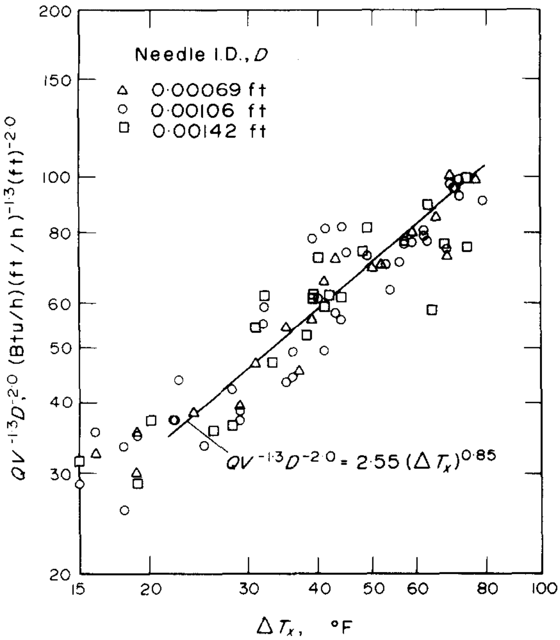

FIG. 4. Dimensional correlation of nucleate boiling heat-transfer data.

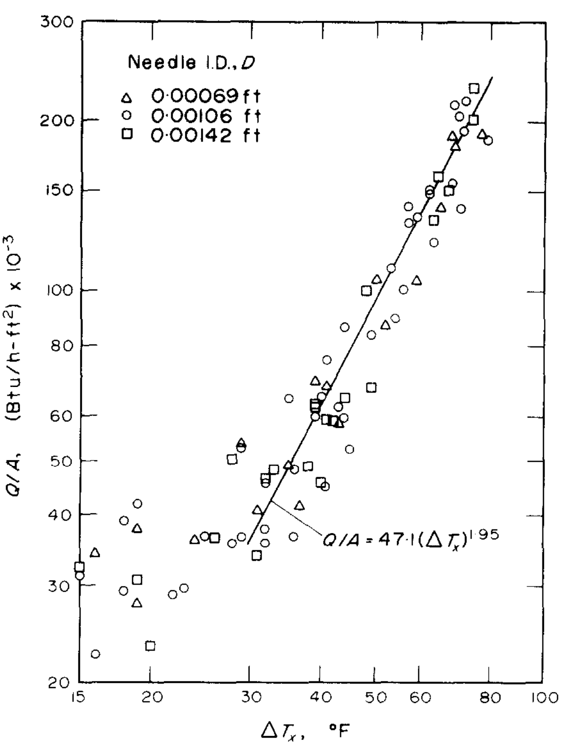

FIG. 5. Dimensional correlation of nucleate boiling heat flux data.

and jet velocity with settings of the heater orientation angle, θ, at 0, 15, 30 and 45 degrees. Examination of the data reveals that no effect of heater orientation angle was noticeable over the range 0 to 45 degrees, and equations (4) and (5) may be used to predict the heat transfer and heat flux.

Comparison of equations (4) and (5) also indicates that the effect of jet velocity and needle diameter are only important insofar as they affect the area of contact. In this sense, they may be thought of as having purely "flow-field" effects rather than heat-transfer effects.

Equations (4) and (5) can be used to predict the heat transfer and heat flux during jet boiling of Freon-113 under the conditions of these experiments. For application to other liquids under different test conditions, these formulas must be extended to include the pertinent physical quantities governing the jet boiling phenomena. Towards this end, the generalized nucleate pool-boiling correlation of Rohsenow [11] was employed. This formula has been used successfully to consolidate a wide range of test data for a number of fluids, and is given by:

$$\frac{c_{p,f}\,\Delta T_x}{h_{fg}} = C_{sf}\left\{\frac{Q/A}{\mu_f h_{fg}}\left[\frac{g_c\sigma_f}{g(\rho_f-\rho_v)}\right]^{0\cdot5}\right\}^{0\cdot33} Pr^{1\cdot7}. \tag{7}$$

Rearranging equation (7):

$$\frac{Q/A}{\mu_f h_{fg}}\left[\frac{g_c\sigma_f}{g(\rho_f-\rho_v)}\right]^{0\cdot5} = \left[\frac{1}{C_{sf}}\left(\frac{c_{p,f}\,\Delta T_x}{h_{fg}}\right)Pr_f^{-1\cdot7}\right]^3. \tag{8}$$

Adjusting the exponent of the r.h.s. of equation (8) to yield the same dependency on the saturation temperature excess as that given by equation (5) gives a generalized correlation for nucleate jet boiling heat flux:

$$\frac{Q/A}{\mu_f h_{fg}}\left[\frac{g_c\sigma_f}{g(\rho_f-\rho_v)}\right]^{0\cdot5} = 7{\cdot}94\times10^4\left[\left(\frac{c_{p,f}\,\Delta T_x}{h_{fg}}\right)Pr_f^{-1\cdot7}\right]^{1\cdot95} \tag{9}$$

where the constant C_{sf} is evaluated in conjunction with the fluid properties to satisfy equation (5). The exponent 1·95 of the ΔT_x term of equation (9) is very nearly equal to that obtained experimentally by Kopchikov *et al.* [8] for liquid boiling in a thin film. In that work, the authors found that the heat flux was dependent on the saturation temperature excess to the 2·0 power. This feature was attributed to the fact that agitation due to vapor bubbles is less pronounced in a thin film than in pool boiling. More specifically, they concluded that after the initial period of growth, the outer surface of a bubble goes beyond the film boundaries and hence the mechanical energy of the bubble growth (unlike pool boiling conditions) is almost unused for intensification of the heat transfer. It appears likely that this same phenomena also occurs in the thin layer of liquid on the area of contact during nucleate jet boiling. The fact that jet velocity and needle diameter only affect area of contact also indicates that the nucleate boiling results should be in agreement with boiling of thin liquid films. Although there is agreement with the exponent on ΔT_x between the present work and [8], surface cavity size distributions undoubtedly play a role in the determination of this exponent but comparative information was not available on surface topology.

The generalized heat flux given by equation (9) is compared in Fig. 6 with the results of Copeland [4]

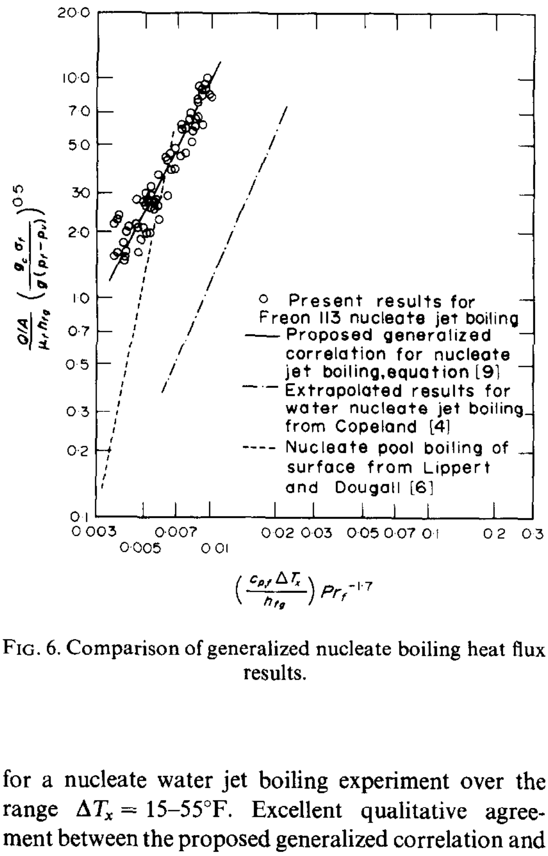

FIG. 6. Comparison of generalized nucleate boiling heat flux results.

for a nucleate water jet boiling experiment over the range $\Delta T_x = 15$–$55°F$. Excellent qualitative agreement between the proposed generalized correlation and the water jet boiling data is obtained, with only a small difference in the slope of the lines being found (2·3 vs 1·95 in the present work). The difference between the two levels indicates that the constant in equation (9) is most probably a function of the particular fluid-surface combination as is the analogous constant, C_{sf}, in the Rohsenow correlation, equation (7). A tabulation of C_{sf} values for Rohsenow's correlation for twelve different fluid–surface combinations given in [12] shows a range of C_{sf} from 0·0027 to 0·015. Noting that the ordinate of Fig. 6 is dependent on C_{sf} to the minus third power, the above range of C_{sf} values thus corresponds to ordinate values different by a factor of $(0{\cdot}0027/0{\cdot}015)^{-3} = (0{\cdot}18)^{-3} = 171$. Hence it is quite plausible for the difference in ordinate values seen in Fig. 6 for the two jet boiling experiments to be caused by the difference in the two constants related to the fluid–surface combinations.

Also shown in Fig. 6 are the results of Lippert and Dougall for nucleate pool boiling of Freon-113 on a copper surface. Good agreement between the proposed correlation and these results is seen to exist. The difference between the slopes of the lines was explained earlier, and the discrepancy between ordinate values is again attributed to the difference between the experimentally determined constants due to different fluid–surface combinations (Freon-113/nickel vs Freon-113/copper).

Deriving a generalized correlation for the heat transfer data, there results in the equation:

$$\frac{Q/D^2}{\mu_f h_{fg}}\left[\frac{g_c \sigma_f}{g(\rho_f-\rho_v)}\right]^{0.5} = 3{\cdot}97 \times 10^6 \left[\left(\frac{c_{p,f}\Delta T_x}{h_{fg}}\right) Pr_f^{-1.7}\right]^{0.85} \times \left(\frac{\mu_f V}{\sigma_f g_c}\right)^{1.3} \quad (10)$$

where the constant ($3{\cdot}97 \times 10^6$) was calculated so that agreement is obtained with equation (9). The term $(\mu_f V/\sigma_f g_c)$ is a dimensionless ratio of the saturated liquid Weber number, $We_f = (\rho_f V^2 D/\sigma_f g_c)$, and the saturated liquid Reynolds number, $Re_f = (\rho_f VD/\mu_f)$, and as such represents a ratio of viscous forces to surface tension forces.

The water jet nucleate boiling heat transfer data of Copeland [4] were correlated showing no effect of jet velocity and jet diameter, whereas the data of the present research show definite effects of these two variables, as given by equation (4) or equation (10). It is quite possible that the corrosion formation noted by that author became the governing mechanism for the spread of the liquid on the test surface, overshadowing the effects of jet velocity and jet diameter.

Equations (9) and (10) are thus recommended for use with other liquids and test conditions in lieu of more specific design data.

Film boiling

Stable film boiling data were obtained in the saturation temperature excess range of 108–608°F. No data were taken in the region of unstable film boiling, $\Delta T_x = 81$–$107°F$. All of the film boiling runs had the same characteristic flow pattern on the surface, with the liquid leaving the surface as a conical spray, as shown in Fig. 7. This phenomenon was also observed by Copeland [4] for film boiling of a water jet. The angle that the conical spray formed with the test surface

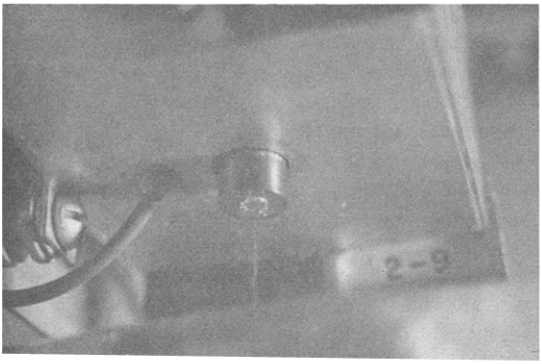

FIG. 7. Photographic view of film boiling. $V = 17400$ ft/h (1·47 m/s); $D = 0·00106$ ft (0·323 mm); $\theta = 0$ degrees; $Q = 17·5$ Btu/h (5·13 W); $Q/A = 73200$ Btu/h-ft^2 (230·9 kW/m^2); $\Delta T_x = 224$°F (124·4°C).

was observed to be a function of the jet velocity, but not of nozzle inside diameter, test surface temperature, or test surface orientation. As the jet velocity increased, the angle between the conical spray and the test surface decreased, as did the size of the droplets in the spray.

The film boiling heat transfer and heat flux data were correlated in the same manner as that described for the nucleate boiling data in the previous section. A dimensional film boiling heat-transfer correlation is presented in Fig. 8. It can be seen that the test data are represented within 24 per cent by the equation:

$$QV^{-0·6}D^{-0·9}\left(\frac{90-\theta}{90}\right)^{-0·5} = 0·965(\Delta T_x)^{0·60}. \quad (11)$$

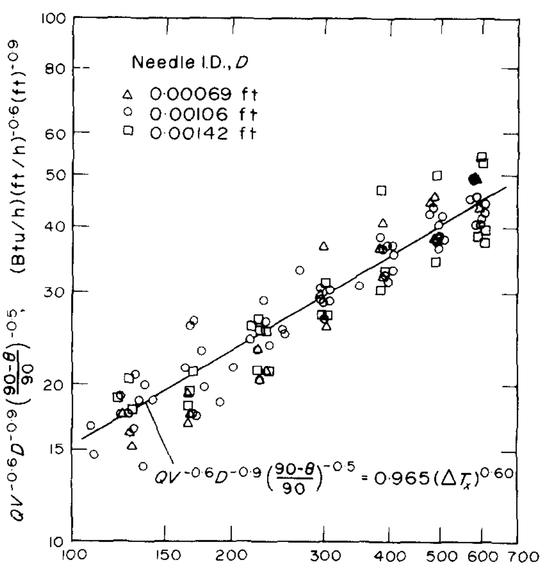

FIG. 8. Dimensional correlation of film boiling heat-transfer data.

The term $(90-\theta/90)$ can be interpreted as the dimensionless ratio of the angle of impact to a normal impact angle.

Inspection of equation (11) reveals that increasing jet velocity, nozzle inside diameter, and test surface temperature each serves to increase the heat transfer, while increasing the test surface orientation angle serves to decrease the heat transfer.

The film boiling heat flux correlation is depicted in Fig. 9 and the test data were correlated within 35 per cent by the equation:

$$(Q/A)V^{-0·5} = 157(\Delta T_x)^{0·25}. \quad (12)$$

It should be noted that no effect of nozzle inside diameter is observed in the above expression.

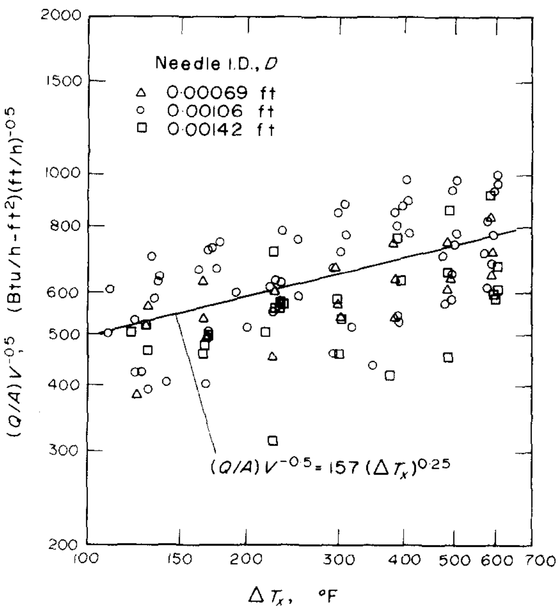

FIG. 9. Dimensional correlation of film boiling heat flux data.

Division of equation (11) by equation (12) yields an expression for the film boiling contact area:

$$A = 6·15 \times 10^{-3}V^{0·1}D^{0·9}\left(\frac{90-\theta}{90}\right)^{0·5}(\Delta T_x)^{0·35}. \quad (13)$$

Inspection of equations (11–13) indicates that the jet velocity has only a weak effect ($V^{0·1}$) on the contact area, although it has considerably stronger effect on the heat transfer and heat flux ($V^{0·6}$ and $V^{0·5}$, respectively). From this it is concluded that during film boiling the effects of the jet velocity are primarily related to the transferral of heat and only slightly related to the contact area. On the other hand, the jet nozzle diameter and test surface orientation appear to have only flow-field effects since they do not show up in the heat flux correlation.

While equations (11) and (12) provide useful design information for Freon-113, it may be helpful to express this information in terms of dimensionless groups which may be useful with other fluids in the absence of specific experimental data. Using the Rayleigh method to obtain the groups, and adjusting the constants and exponents to match the present data gives:

$$\frac{Q}{\mu_v h_{fg}}\left(\frac{\mu_v^2}{\rho_v^2 g}\right)^{-0\cdot33} = 893\left[\left(\frac{\rho_v}{\mu_v g}\right)^{0\cdot33} V\right]^{0\cdot6}\left[\left(\frac{\mu_v^2}{\rho_v^2 g}\right)^{-0\cdot33} D\right]^{0\cdot9} \times\left(\frac{90-\theta}{90}\right)^{0\cdot5}\left(\frac{k_v \Delta T_x}{\mu_v h_{fg}}\right)^{0\cdot6} \quad (14)$$

$$\frac{Q/A}{\mu_v h_{fg}}\left(\frac{\mu_v^2}{\rho_v^2 g}\right)^{0\cdot33} = 1{\cdot}35\left[\left(\frac{\rho_v}{\mu_v g}\right)^{0\cdot33} V\right]^{0\cdot5}\left(\frac{k_v \Delta T_x}{\mu_v h_{fg}}\right)^{0\cdot25}. \quad (15)$$

CONCLUSIONS

Based on the results of this experimental investigation, the following conclusions are drawn:

1. The heat transfer, heat flux, and area of contact during nucleate boiling of an impinging liquid jet are all independent of the orientation of the heater surface over the range of 0 to 45 degrees relative to horizontal.
2. Nucleate boiling heat flux is further independent of the jet velocity and nozzle inside diameter, being dependent solely on the saturation temperature excess. Thus the jet velocity and nozzle inside diameter only serve to increase the area of contact and, as a result, the heat transfer during nucleate boiling.
3. The film boiling heat flux is independent of jet nozzle diameter and test surface orientation, although the heat transfer and contact area are dependent on these variables.
4. The jet velocity has only a minor effect on the contact area during film boiling for the range of velocities studied here.

Acknowledgement—The support of the National Science Foundation through Grant GK-24637 is gratefully acknowledged.

REFERENCES

1. A. D. Akimenko, Features of film boiling in surface water cooling, NASA Report TT-F-10184, N66-33689 (1966).
2. Surface tension of the "Freon" compounds, Dupont Freon Technical Bulletin D-27, Wilmington, Delaware, 1967.
3. A. F. Benning and R. C. McHarness, Thermodynamic properties of "Freon-113" trichlorotrifluorethane CCl_2F–$CClF_2$ with addition of other physical properties, DuPont Freon Technical Bulletin T-113A, Wilmington, Delaware (1938).
4. R. J. Copeland, Boiling heat transfer to a water jet impinging on a flat surface (−1 g), Ph.D. dissertation, Southern Methodist University (1970).
5. R. C. Downing, Transport properties of "Freon" fluorocarbons, DuPont Freon Technical Bulletin C-30, Wilmington, Delaware (1967).
6. T. E. Lippert and R. S. Dougall, A study of the temperature profiles measured in the thermal sublayer of water, Freon-113 and methyl alcohol during pool boiling, *J. Heat Transfer* **90**, 347–352 (1968).
7. J. G. Knudsen and D. L. Katz, *Fluid Dynamics and Heat Transfer*. McGraw-Hill, New York (1958).
8. I. A. Kopchikov, G. I. Vornin, T. A. Kolachi, D. A. Tabrintosv and P. D. Lebedeb, Liquid boiling in a thin film, *Int. J. Heat Mass Transfer* **12**, 791–796 (1969).
9. R. G. Nevins, Jr., The cooling power of an impinging jet, Ph.D. Dissertation, University of Illinois (1953).
10. P. C. Reynard and W. J. Billerbeck, Nethan III, Thermal Network Analyzer Program, TRDS/165 (1967).
11. W. M. Rohsenow, A method of correlating heat-transfer data for surface boiling of liquids, *Trans. Am. Soc. Mech. Engrs* **74**, 969–976 (1952).
12. W. M. Rohsenow, Heat transfer with boiling, in *Developments in Heat Transfer*, edited by W. M. Rohsenow, pp. 169–260. The M.I.T. Press, Cambridge, Massachusetts (1964).

TRANSFERT THERMIQUE PAR EBULLITION POUR UN JET DE FREON 113 FRAPPANT VERS LE HAUT UNE SURFACE PLANE ET CHAUFEE

Résumé—On a obtenu des résultats expérimentaux sur le transfert de chaleur et le flux thermique pour un jet frappant une surface chauffée, en régime d'ébullition nucléée et en film. Les variables sont le diamètre intérieur de la tuyère, l'orientation et la température de la surface. On a trouvé une formule générale pour le flux thermique en ébullition nucléée, en utilisant une forme modifiée de l'équation de Rohsenow pour l'ébullition en réservoir. Pour le fréon 113, des expressions dimensionnelles du transfert de chaleur et du flux, à la fois pour l'ébullition nuclée et en film, ont été obtenues en fonction des quatre variables caractéristiques.

WÄRMEÜBERGANG BEIM SIEDEN EINES VON UNTEN AUF EINE EBENE HEIZFLÄCHE AUFTREFFENDEN FREON-113-STRAHLS

Zusammenfassung—Der Wärmeübergangskoeffizient und die Wärmestromdichte bei einem auf eine beheizte Versuchsplatte auftreffenden Strahl wurden im Bereich des Blasen- und Filmsiedens experimentell untersucht. Unabhängige Versuchsvariablen waren der Innendurchmesser der Strahldüse, die Neigung der Heizfläche und die Heizflächentemperatur. Mit Hilfe einer modifizierten Form der Rohsenow-Gleichung konnte die Wärmestromdichte beim Blasensieden des Strahls in verallgemeinerter Weise korreliert werden.

Für Freon-113 konnten sowohl für den Bereich des Blasensiedens wie des Filmsiedens dimensionslose Beziehungen für den Wärmeübergangskoeffizienten und die Wärmestromdichte in Abhängigkeit von den vier Versuchsparametern aufgestellt werden.

ТЕПЛОПЕРЕНОС ПРИ КИПЕНИИ СТРУИ ФРЕОНА-113, НАПРАВЛЕННОЙ ВВЕРХ НА ПЛОСКУЮ НАГРЕВАЕМУЮ ПОВЕРХНОСТЬ

Аннотация — Проведены экспериментальные измерения теплообмена и теплового потока к струе, направленной на нагреваемую рабочую поверхность, в условиях пузырькового и пленочного кипения. Рабочими параметрами были внутренний диаметр сопла, ориентация и температура рабочей поверхности. Данные по тепловому потоку в струе при пузырьковом кипении обобщались с помощью модифицированного уравнения Розенау для кипения в большом объеме. Для теплового потока и теплообмена при пузырьковом и пленочном кипении фреона-113 получены размерные соотношения, включающие четыре рабочих параметра.